Results in Engineering 24 (2024) 103155

Contents lists available at ScienceDirect

Results in Engineering

journal homepage: www.sciencedirect.com/journal/results-in-engineering

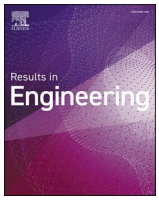

Stability of long uniform slopes in cohesionless soils with seepage parallel to slope surface

Ghassan Abou-Samra [a,*], Vincenzo Silvestri [b]

[a] University of Moncton, Moncton, New Brunswick, Canada
[b] Ecole Polytechnique, Montreal, Quebec, Canada

ARTICLE INFO

Keywords:
Landslides
Earth retention systems
Rankine
Saturated infinites slopes
Cohesionless soils

ABSTRACT

A method is employed in this paper for the computation of earth pressures mobilized by landslides in cohesionless soil slopes against retention systems. For calculation purposes, the water table is taken to be parallel to the slope and at a depth z_w. Steady seepage is assumed to be taking place in a direction parallel to the slope. End effects are taken into account. In the upper part of the slope, the soil is considered to be in a Rankine active state of equilibrium and a Rankine passive state of equilibrium is assumed to reign in the lower part of the slope. The infinite slope concept is applied to the central part of the slope. The theory shows that the slip surfaces below the water table are curved, not straight lines.

The theoretical procedure developed in the present paper was applied to the analysis of an initially unstable long slope that failed in spite of the presence of a shear pile wall made up of a row of closely spaced 1m-diameter bored piles. The retaining system was designed based on the Rankine active state of equilibrium, using a factor of safety of about 1.7. It is shown that, as the shear pile wall was located in the lower part of the slope, it was subjected to a much greater force, compatible with a Rankine passive state of equilibrium, corresponding to a factor of safety of about 0.9. As a result, the shear pile wall was doomed to fail.

1. Introduction

The basic principles that govern the design and construction of stable slopes are well established. Approaches to their design can be categorized as follows: a) avoid the problem, b) reduce the forces tending to cause movements, and c) increase the forces resisting movements [1,2]. The techniques used in the latter approach, which are of particular interest in the context of this paper, function either by applying a resisting force or by increasing the internal strength of the soils in the failure zone. The most common structural retention systems that are employed to increase resisting forces include conventional retaining walls, shear keys, externally braced walls or walls supported by anchors and tiebacks, piles, and drilled shafts [1,3]. Structural retention systems have sometimes failed for two main reasons: either the forces applied by the sliding mass were underestimated, or the sliding mass simply bypassed the retaining structure [3,4].

As the lateral extent of the slopes treated in the present paper is very large compared with the depth of the slip surfaces, the slopes will be considered of infinite extent. In such context the infinite slope analysis procedure, which is rigorous and valid for cohesionless soils, is also applicable to other cases where the slip surface is parallel to the slope face with the depth of the slip surface being small compared with the lateral dimension of the slope [5].The latter condition may exist when there is a stronger layer of soil at shallow depth; for example, where a layer of weathered soil exists near the surface of the slope and is underlain by a stronger, unweathered substratum, as discussed later in the paper.

The stability analysis of infinite slopes is considered the first step in understanding the mechanics of slope stability, supported by the fact that most textbooks and design manuals in soil mechanics and geotechnical engineering include this topic [5–8]. Despite being one of the oldest techniques of earth pressure determination [9,10], infinite slope analysis is very useful, particularly for analyzing shallow landslides where the depth of the slip surface is very small compared with the lateral extent of the slope [5]. Lately, this approach has attracted renewed attention with a diversity of extensions to various geotechnical problems such as nonhomogeneous soil profiles [11], partially saturated soils and rainfall infiltration [12,13], seismic acceleration [14], elastic-plastic response [15,16], slope volume and geometry [17], and bonded soils and rocks with particular characteristics [18–21].

The stability of long uniform slopes in cohesionless soils, inclined at

* Corresponding author.
E-mail addresses: ghassan.abou-samra@umoncton.ca (G. Abou-Samra), vincenzo.silvestri@polymtl.ca (V. Silvestri).

https://doi.org/10.1016/j.rineng.2024.103155
Received 14 August 2024; Received in revised form 6 October 2024; Accepted 12 October 2024
Available online 15 October 2024

Nomenclature:

c	cohesion
c'_p	effective peak cohesion
c'_{res}	effective residual cohesion
F	factor of safety
F_p	maximum force applied to retention system
F_{rp}	passive force
H	depth of retention system
k_{ra}	Rankine active pressure coefficient
L	length of landslide
L'	length of central part of landslide
L_B	length of passive end of landslide
L_{crit}	critical length of landslide $= L' + L_B$
u	porewater pressure
z	depth
z_w	depth of water table
α	angle between slope surface and slip surface
β	inclination angle of slope
γ	unit weight
γ_{sat}	saturated unit weight
γ_w	unit weight of water
γ'	effective unit weight $= \gamma_{sat} - \gamma_w$
ε	angle between slope surface and plane through center of Mohr circle and pole
θ_1, θ_2	angles between vertical direction and failure surfaces
ϕ	friction angle
ϕ'_p	effective peak friction angle
ϕ'_{res}	effective residual friction angle
σ_n	normal stress on plane parallel to slope surface
σ'_n	effective normal stress on plane parallel to slope surface
σ_{ra}	total Rankine active pressure on vertical plane
σ_{rp}	total Rankine passive pressure on vertical plane
σ_v	total vertical stress on plane parallel to slope surface
τ	applied shear stress on plane parallel to slope surface
τ_f	shear resistance on plane parallel to slope surface
$\Delta\tau$	shear deficit at z on plane parallel to slope surface $= \tau - \tau_f$

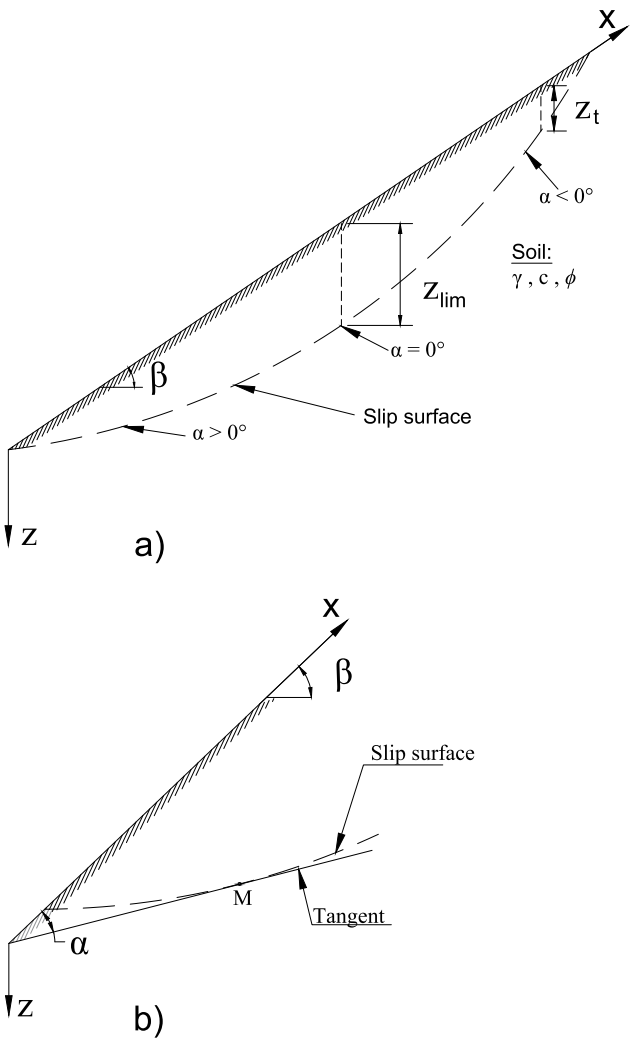

Fig. 1. Frontard's solution for $\beta > \varnothing$: a) Slip surface; b) Definition of angle α (adapted from Ref. [22]).

an angle β with respect to the horizontal less than the friction angle ϕ of the soil, is analyzed using the concept of an infinite slope. In such case it is assumed that the potential failure surface is parallel to the surface of the slope and at a depth that is small compared to the length of the slope. The slope is then considered as being of infinite length, with end effects being ignored. When the slope is dry or when the water table coincides with the surface of the slope, that is, when the pore water pressures are proportional to the depth of the slide, the direction of the failure surface remains constant with depth [8]. However, when the water table is located at some depth below the surface of the slope, the direction of the potential failure plane varies with depth below the water table.

For calculation purposes in the context of the present paper, the water table is taken to be parallel to the slope and at a depth z_w. Steady seepage is assumed to take place in a direction parallel to the slope. End effects are taken into account. Thus, while in the upper part of the slope, the soil is in a Rankine active state of equilibrium, a Rankine passive state of equilibrium reigns in the lower part of the slope. In addition, the infinite slope concept is applied to the central part of the slope. The theory shows that the slip surfaces below the water table are curved, not straight lines as one would have expected from application of Rankine conditions to dry cohesionless soils.

The present paper also presents a case history that involves a landslide triggered by cuts made at the toe of a long slope for the construction of a highway and a secondary road. The landslide occurred in spite of the presence of a row of closely spaced large diameter piles installed for remediation purposes. Results of stability analyses show that the shear pile wall was unable to resist the forces mobilized by the landslide. A preliminary analysis of the landslide was made by Silvestri and Tabib [22].

2. Theoretical approach

Résal [23] determined the stresses, the directions of the failure surfaces, and the equations of the slip surfaces in long cohesive-frictional slopes, by assuming that Rankine's conditions prevailed. This implies that the vertical stress σ_v, acting at the depth z on a plane parallel to the slope in everywhere equal to $\gamma z cos\beta$, where γ is the unit weight of the soil and β is the inclination angle of the slope with respect to the horizontal. Frontard [24] integrated Résal's equations and obtained an expression for the slip surface for $\beta > \phi$ (See Fig. 1a). In addition, Frontard [24] showed that while the upper part of the slope was in a state of active equilibrium, the corresponding lower part was in a passive state. These

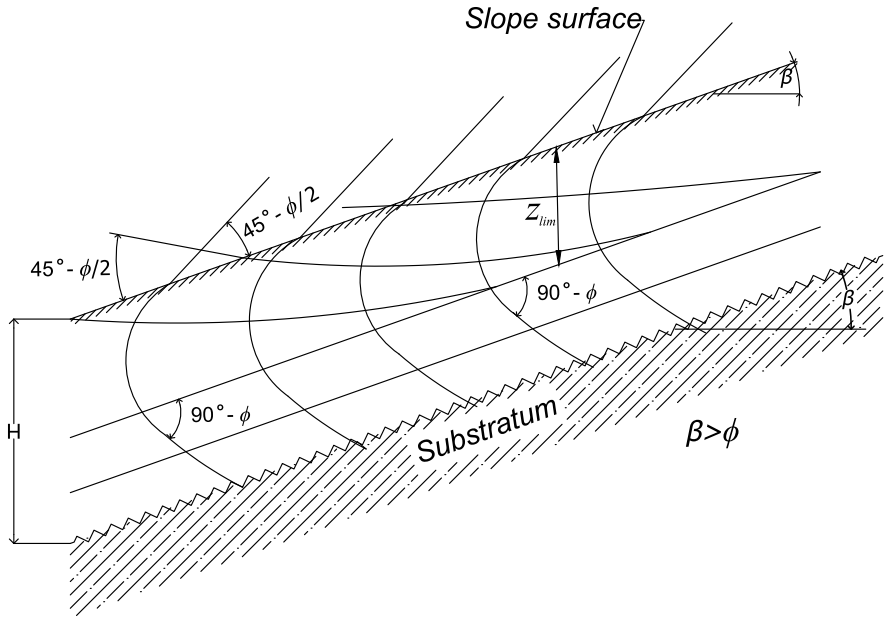

Fig. 2. Slip line field at passive end of landslide (modified after [25]).

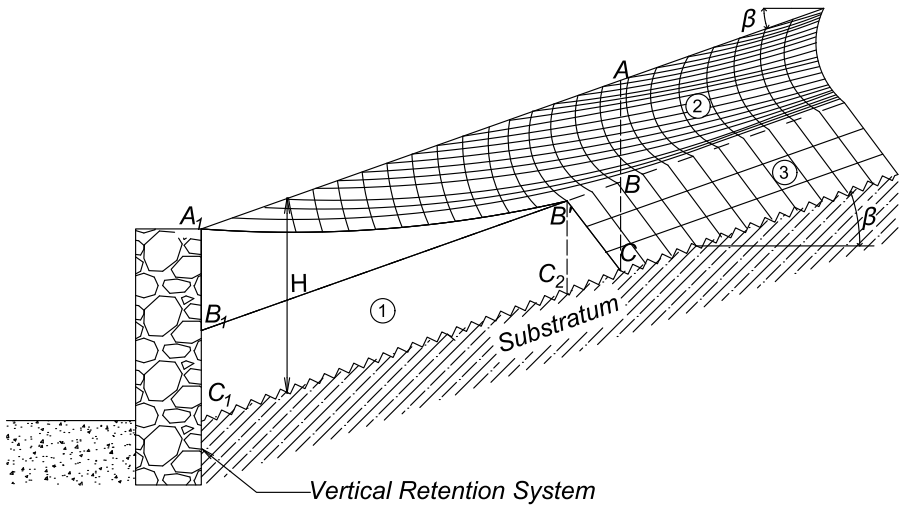

Fig. 3. Mixed elastic-plastic zones at passive end of landslide (modified after [25]).

two states are characterized by different values of the angle α shown in Fig. 1b. The passive zone corresponds to $\alpha \geq 0$ and the active zone to $\alpha < 0$, as shown in Fig. 1a. Résal [23] also showed that there existed a limiting height z_{lim}, corresponding to $\alpha = 0$, for which a long slope could not remain stable if its height $H > z_{lim}$.

Fig. 2 presents a typical slip line field at the lower or passive end of a landslide in a cohesive–frictional soil [25]. Because the height $H > z_{lim}$ in the context of the present study, it is assumed that a vertical retention system is present to stabilize the landslide. The slip lines reported in Fig. 2 follow Résal's solution for $H \leq z_{lim}$ in the passive zone. But for $z > z_{lim}$, one family of slip lines is parallel to the slope surface, whereas the other is inclined at $\left(90^{O} - \phi\right)$ to the first one.

Fig. 3 presents a section at the lower end of a landslide, adjacent to a vertical retention system. Following Sanglerat et al. [25], it is possible to admit the existence of a mixed elastic-plastic equilibrium diagram that consists of three zones, namely, one zone in elastic equilibrium (zone 1), and two plastic zones: zone 2 in Rankine passive state for $z \leq z_{lim}$, and zone 3 in limit equilibrium for $z > z_{lim}$.

Concerning infinite slopes in dry cohesive-frictional soils, when a stability analysis is made by assuming that the potential failure plane is parallel to the slope surface, the factor of safety F is calculated by comparing the shear resistance $\tau_f = c + \sigma_n \tan\phi = c + \gamma z(\cos\beta)^2 \tan\phi$ to the applied shear stress $\tau = \gamma z \sin\beta \cos\beta$, resulting in

$$F = \frac{c + \gamma z(\cos\beta)^2 \tan\phi}{\gamma z \sin\beta \cos\beta} \tag{1a}$$

For $c = 0$, Eq. (1a) reduces to

$$F = \frac{\tan\phi}{\tan\beta} \tag{1b}$$

According to this equation, when $F = 1$, any plane parallel to the slope surface is a failure plane. When the water table is uniformly

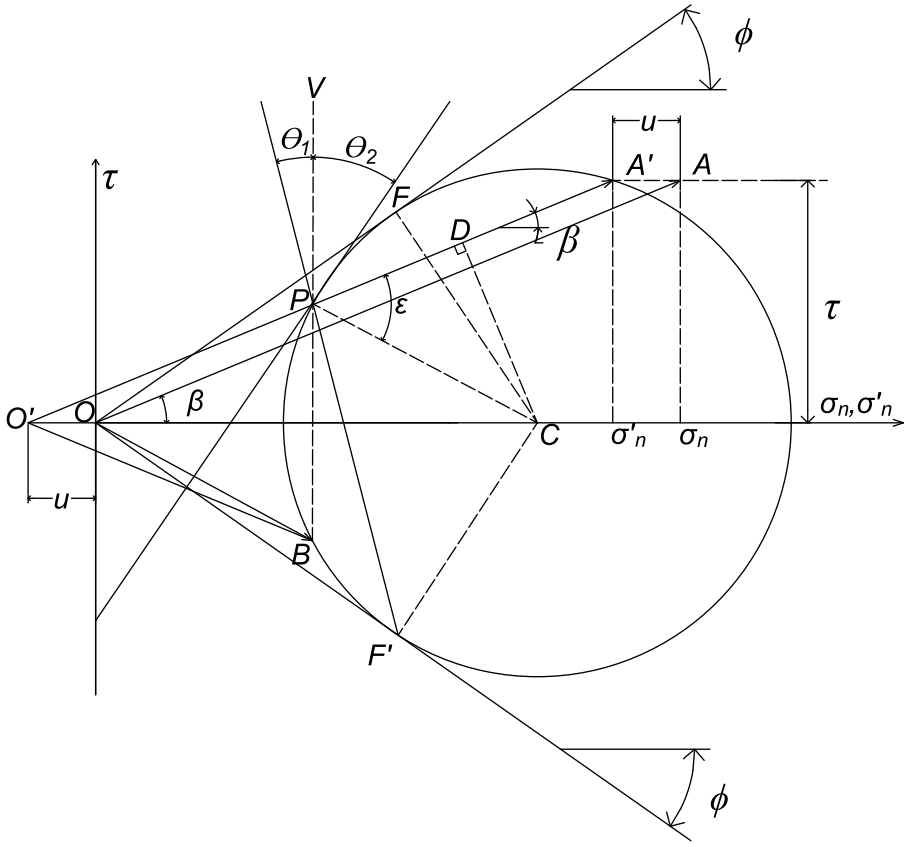

Fig. 4. Active case.

located at a depth z_w below the slope surface, Eqs. (1a) and (1b) become respectively

$$F = \frac{c + [\gamma z_w + (z - z_w)(\gamma_{sat} - \gamma_w)](\cos\beta)^2 \tan\phi}{[\gamma z_w + \gamma_{sat}(z - z_w)]\sin\beta\cos\beta} \tag{2a}$$

and

$$F = \frac{[\gamma z_w + (z - z_w)(\gamma_{sat} - \gamma_w)](\cos\beta)^2 \tan\phi}{[\gamma z_w + \gamma_{sat}(z - z_w)]\sin\beta\cos\beta} \tag{2b}$$

where γ_{sat} = saturated unit weight of soil below the water table and γ_w = unit weight of water. Note also that $(\gamma_{sat} - \gamma_w) = \gamma'$ represents the effective unit weight of the soil. The pore water pressure $u = \gamma_w(z - z_w)(\cos\beta)^2$. From Eq. (2b), the depth $z = z_{lim}$ of the failure plane is found for $F = 1$, yielding

$$z = z_{lim} = \frac{[(\gamma - \gamma')\cos\beta\tan\phi + (\gamma_{sat} - \gamma)\sin\beta]}{[\gamma_{sat}\sin\beta - \gamma'\cos\beta\tan\phi]} \tag{3}$$

in the case of a cohesionless slope. As a result, a partially submerged infinite slope becomes again unstable if its depth is greater than z_{lim}. While Eqs.1b and 2b apply to the central zone of a long cohesionless slope, failure surfaces in the upper and lower end zones for $z > z_w$ are no longer parallel to the slope surface, similarly to the suggestion made by Résal [23] for purely cohesive slopes.

Consider first the upper end zone where the soil is in a Rankine active state of limit equilibrium, as shown in Fig. 4. The vector OA represents the vertical total stress σ_v, with normal and tangential stress components σ_n and τ. For z less than or equal to z_w, Rankine's theory for dry soil applies entirely. The active pressure σ_{ra} which acts on a vertical plane is parallel to the surface of the slope; it is represented by the vector OB whose magnitude is equal to the distance OP, where P is the pole of the Mohr circle. The angle ε which allows to find the directions of the failure surfaces is constant and equal to $\sin^{-1}(\sin\beta/\sin\phi)$ for z less than or equal to z_w, as shown by Rankine [9]. The directions of the failure planes are given by the angles θ_1 and θ_2 in Fig. 4. While the angle θ_1 on the downhill side is sometimes called the outer plane of rupture, the angle θ_2 on the uphill side is referred to as the inner plane of rupture [10]. These angles are obtained by drawing lines starting from the pole and passing through the failure points F and F' on Mohr circle.

For z greater than z_w, the pore water pressure u must be taken into account. As a consequence, it becomes necessary to determine the effective normal stress $\sigma'_n = \sigma_n - u$ at A, that is A', with the tangential stress τ remaining unchanged. The vector $O'A'$ is parallel to OA and the distance $O'O$ equals the pore water pressure u. The limiting depth z_{lim} corresponds to the point where A' touches the effective stress envelope. For any depth z less than z_{lim}, the total active pressure σ_{ra} acting on a vertical plane is given by the distance $O'B$. Note that $O'B$ equals $O'P$, where P is again the pole.

The active pressure $\sigma_{ra} = \gamma z\cos\beta k_{ra}$ for z less than or equal to z_w, where k_{ra} is the active pressure coefficient which is given by $k_{ra} = \frac{\cos\beta - \sqrt{\sin^2\phi' - \sin^2\beta}}{\cos\beta + \sqrt{\sin^2\phi' - \sin^2\beta}}$. For z greater than z_{lim}, the total active pressure σ_{ra} is given by

$$\sigma_{ra} = O'D - DP \tag{4}$$

where

$$O'D = O'C\cos\beta = (O'O + OC)\cos\beta \tag{5a}$$

$$DP = OC\sin\phi \tag{5b}$$

and

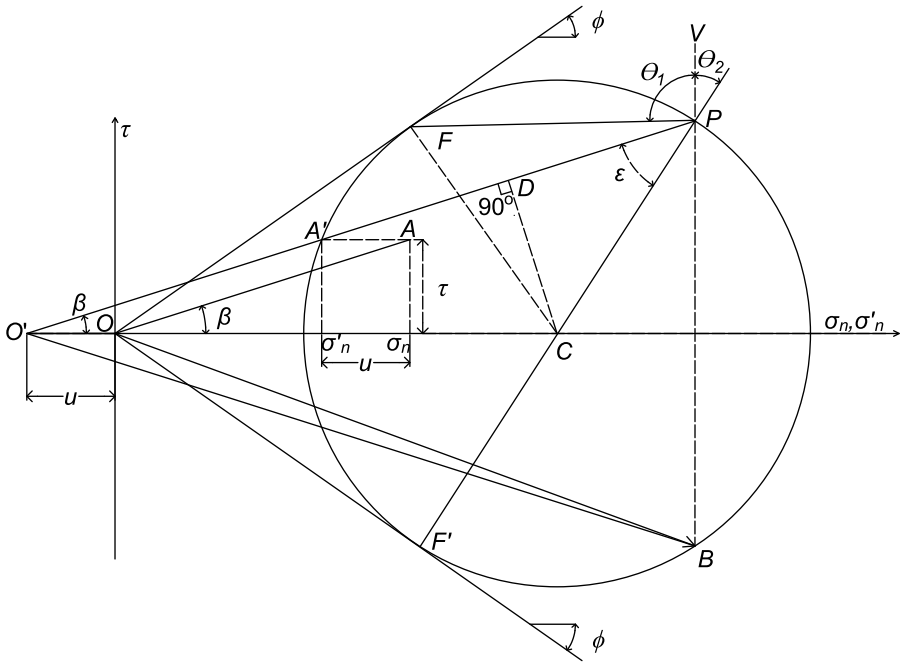

Fig. 5. Passive case.

$$OC = \sec^2\beta\left\{\sigma_n' - \left[(\sigma_n' \sin\phi)^2 + (\tau\cos\phi)^2\right]^{1/2}\right\} \tag{5c}$$

The directions of the failure surfaces which are given by the lines PF′ and PF in Fig. 4 are equal respectively to θ_1 and θ_2 with respect to the vertical, that is,

$$\theta_1 = \frac{(90^o - \phi)}{2} - \frac{(\varepsilon - \beta)}{2} \tag{6a}$$

and

$$\theta_2 = \frac{(90^o - \phi)}{2} + \frac{(\varepsilon - \beta)}{2} \tag{6b}$$

Note the angle ε which is given by

$$\varepsilon = \sin^{-1}\left[\frac{(O'O + OC)\sin\beta}{OC\sin\phi}\right] \tag{7}$$

varies with depth below the water table because the porewater pressure u, which corresponds to $O'O$, is variable; it thus follows that the directions of the failure surfaces also vary as function of depth.

Consider now the lower end zone where the soil is in a Rankine passive state of limit equilibrium, as shown in Fig. 5. Again, the vector OA represents the vertical total stress. In this case, the distance OC is given by

$$OC = \sec^2\beta\left\{\sigma_n' + \left[(\sigma_n' \sin\phi)^2 + (\tau\cos\phi)^2\right]^{1/2}\right\} \tag{8}$$

For any depth less than z_w, the passive pressure which acts on a vertical plane is parallel to the surface of the slope and is given by $\sigma_{rp} = \gamma z\cos\beta\, k_{rp}$, where $k_{rp} = 1/k_{ra}$. In addition, the angle ε is again equal to $\sin^{-1}(\sin\beta/\sin\phi)$. As a consequence, the directions of the failure planes which are given respectively by

$$\theta_1 = \frac{(90^o + \phi)}{2} + \frac{(\varepsilon + \beta)}{2} \tag{9a}$$

and

$$\theta_2 = \frac{(90^o + \phi)}{2} - \frac{(\varepsilon + \beta)}{2} \tag{9b}$$

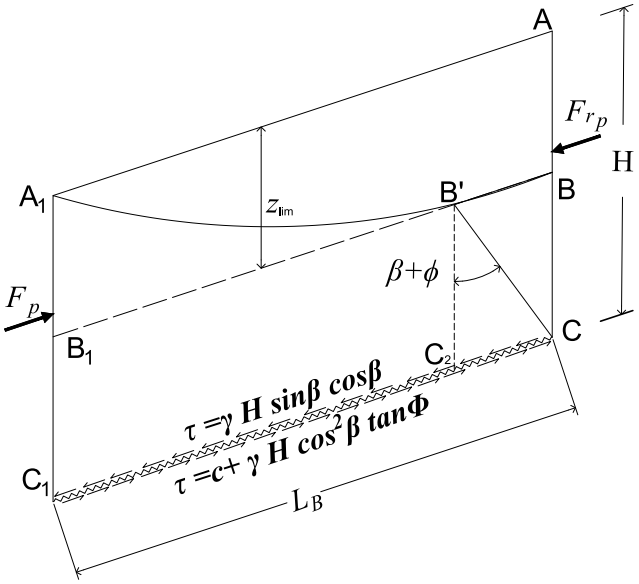

Fig. 6. Free-body diagram of section of cohesive-frictional slope adjacent to retention system (adapted from Ref. [22]).

are constant for z less than z_w.

For any depth z greater than z_w but less than z_{lim}, the total passive pressure σ_{rp} acting on a vertical plane is given by the distance $O'B$ in Fig. 5. Note that $O'B$ equals $O'P$, where P is again the pole. In this case, the total passive pressure σ_{rp} is given by

$$\sigma_{rp} = O'D + DP \tag{10}$$

where $O'D$ and DP are given respectively by Eqs. (5a) and (5b). But, as the angle ε which is given by Eq. (7) is function of the porewater pressure, the directions θ_1 and θ_2 of the failure surfaces, which are still parallel to the lines PF and PF', vary with depth.

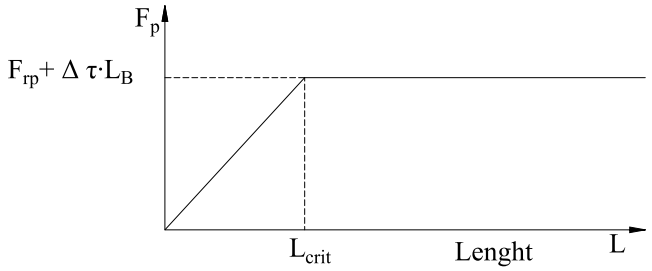

Fig. 7. Simplified relationship between force applied to retention system and length of landslide (adapted from Ref. [26]).

However, for $z > z_{lim}$, as the directions of the failure surfaces are considered to be constant with depth from Fig. 3, the passive earth pressure σ_{rp} may be found from a simple rule of three, that is,

$$\sigma_{rp} \text{ at } z = \frac{z}{z_{lim}}\sigma_{rp} \text{ at } z_{lim} \tag{11}$$

Fig. 6 presents the section of a landslide between a vertical retention system $A_1B_1C_1$ and the vertical plane ABC passing through point C where the first slip line cuts the substratum. Rankine passive force F_{rp} acting on the plane ABC is determined from the earth pressures given by Eq. (10) for $z \leq z_{lim}$, and Eq. (11) for $z > z_{lim}$. The length L' of slope required to mobilize the passive force F_{rp} is obtained from:

$$L' = \frac{F_{rp}}{\Delta\tau} = \frac{F_{rp}}{\gamma H \sin\beta\cos\beta - (c + \gamma H \cos^2\beta \tan\phi)} \tag{12}$$

where the shear deficit $\Delta\tau$ represents the difference between the applied shear stress and the corresponding shear resistance existing at a depth H on the plane parallel to the slope.

The maximum force F_p acting on the vertical retention system is found from the equilibrium of the free-body diagram shown in Fig. 6, that is:

$$F_p = F_{rp} + \Delta\tau.\, L_B \tag{13a}$$

or

$$F_p = F_{rp} + \left[\gamma H \sin\beta\cos\beta - \left(c + \gamma H \cos^2\beta \tan\phi\right)\right].L_B \tag{13b}$$

where the length L_B equals the distance C_1C in Fig. 6. Because $L_B = C_1C_2 + C_2C$, it is necessary to determine separately segments C_1C_2 and C_2C. The length of segment C_1C_2 may be found by simply assuming that the slip line B'A_1 is an arc of circle. As for C_2C, it is given by:

$$C_2C = (H - z_{lim})\frac{\sin(\beta + \varnothing)}{\cos\varnothing} \tag{14}$$

On the basis of the global equilibrium of a sliding mass of total length L, the minimum force acting on the vertical retention system is:

$$F_{min} = \Delta\tau.L = \left[\gamma H\, sin\,\beta\cos\beta - \left(c + \gamma H\, cos^2\,\beta\, tan\varnothing\right)\right] \tag{15}$$

However, such force cannot be greater than the force F_p found from Eq. (13).

Two solutions will ensue.

a) When $L > L' + L_B = L_{crit}$, the landslide will pass over the retention system, even if the wall is stable. The force mobilized by the sliding mass corresponds to F_p.
b) When $L \leq L' + L_B = L_{crit}$, the landslide is stabilized by the retention system, provided that the system is designed to resist the applied force. This force is less than F_p but greater than or equal to F_{min}. The simple relationship shown in Fig. 7 may be used to determine the actual force.

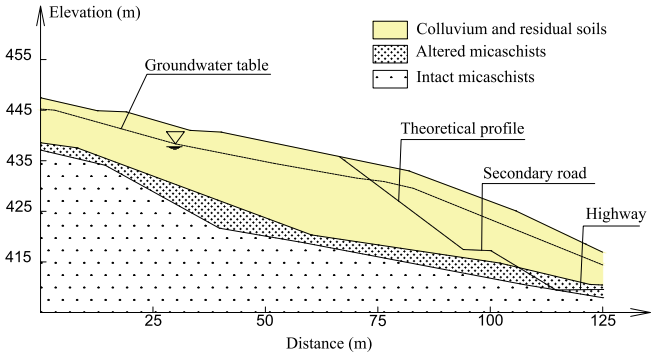

Fig. 8. Case history (modified after [26]).

3. Case history

Fig. 8 illustrates the stratigraphy and the geometry of the case history at study, which was first analyzed by Blondeau & Virollet [26]. It is re-analyzed in the present paper for obtaining a clearer picture of both the mechanisms involved in the landslide and the mobilized earth pressures which led to the failure of the retention system.

As shown in Fig. 8, excavations were made at the lower end of a long slope, inclined at an average angle of 18° with respect to the horizontal, for construction of a highway and a secondary road. The overburden which consists of colluvium and residual soils is underlain by 4*m* thick layers of altered micaschists resting on sound bedrock. The bedrock surface is approximately parallel to the slope surface, at a depth of 7*m* to 8*m*. The ground water is parallel to the surface, at a depth varying from 2.5*m* to 3*m*.

A first landslide was triggered during the initial stages of the excavations. Distress manifested in the form of transverse cracks 40*m* upslope of the earthworks, with movements being relatively minor. Two to three months later, when the earthworks were halted, a second crack appeared 20 m upslope of the first one. Still, the movements were small. Subsequently, the work resumed and the final excavation levels were successfully reached by reducing the inclination of the slopes. Unfortunately, a general landslide occurred sometime later, destroying the secondary road and the upper slope of the highway. The contractor decided to build a shear pile wall to preserve the highway platform and to stop the landslide movements. The wall consisted of a single row of closely spaced 1 m diameter concrete piles which were to be anchored in the intact rock. However, not all the piles reached the bedrock, because of construction difficulties. The pile heads were tied together by a massive 2*m* square cap beam. According to Blondeau and Virollet [26], the shear pile wall was designed to withstand an ultimate load of 590 kN/m, which was based upon Rankine active earth pressures. As these authors mention that the active force was estimated at 350 kN/m, the design of the wall implied a factor of safety of about 1.7. In spite of the shear pile wall, landslide movements progressed, with the sliding mass finally passing over the crest of the wall at several places. The cap beam was eventually displaced by more than 0.7*m*. The total length of the slope involved in the landslide measured 110*m*.

The gravelly and heterogeneous nature of the soils involved in the landslide prevented the performance of laboratory strength tests for the determination of effective strength parameters. However, as the geometry of the landslides and the pore water pressures were determined quite accurately during and after the landslide movements, Blondeau and Virollet [26] were able to obtain reasonable estimates of the effective strength parameters, by carrying out stability analyses. Blondeau & Virollet [26] obtained peak strength parameters, $c'_p = 5\ kPa$, $\phi'_p = 22°$, for the initial first-time landslide, and residual strength parameters, $c'_p = 0$, $\phi'_{res} = 20°$, for the subsequent re-activation of the landslide. The values of both sets of strength parameters (i.e., peak and

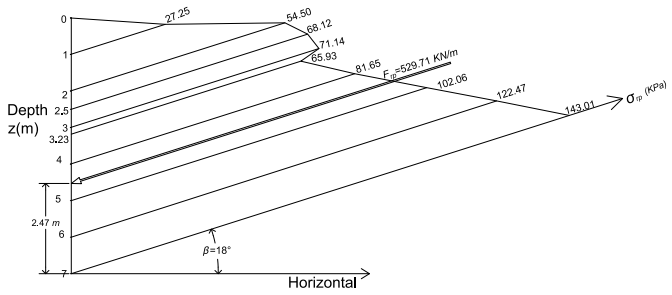

Fig. 9. Pressure distributions and forces on vertical plane at passive end of landslide.

residual) are quite similar to triaxial and direct shear test results obtained by Blondeau & Josseaume [27] on both intact and pre-cut soil specimens recovered from the sites of several landslides in the same region.

Concerning the unit weights of the soils, a value of $21kN/\ m^3$ based on local experience, was retained for both γ and γ_{sat}. The groundwater table was found at a depth of $2.5m$ at the time of the general landslide. The minimum thickness H of the soils involved in the landslide was $7m$, with the failure surface being confined to the boundary between the overburden and the altered micaschists. The factor of safety F for a first-time slide, applicable to an infinite slope, is found to be 0.98 from Eq. (2a), with $c'_p = 5\ kPa$, $\phi'_p = 22°$, $\gamma = \gamma_{sat} = 21kN/m^3$, $\gamma_w = 10kN/\ m^3$, $z_w = 2.5m$, $H = 7m$, and $\beta = 18°$. The slope was thus marginally safe, prior to the start of earthworks. In proceeding as per Eq. (2), the infinite slope analysis ignores the driving force at the upper or active end of the landslide and the resisting force at the lower or passive end. Because the resisting force is generally greater than the driving force, such analysis leads to a conservative result [1].

For comparison purposes, stability analyses involving circular failure surfaces were also carried out by Blondeau and Virollet [26]. It was found that when the initial excavation reached a depth of about $6m$, a factor of safety of one was obtained based upon the peak effective strength parameters $c'_p = 5\ kPa$, $\phi'_p = 22°$, with the lowest point on the failure circle located $3m$ below the excavated platform. Additional circular failure analyses were completed using the residual effective strength parameters $c'_{res} \approx 0$, $\phi'_{res} = 20°$. A factor of safety of one was obtained for a series of failure circles involving a much larger volume of soil. The lowest points on these failure circles were about $6m$ below the excavated platform.

As mentioned above, landslide movements increased considerably during the progression of the earthworks. It is thus believed that the effective strength parameters reached their residual values during the general landslide. Because Blondeau and Virollet [26] deduced that failure analyses based upon the residual values $c'_{res} \approx 0$, $\phi'_{res} = 20°$ agreed with the observed response, the soil would thus behave like a cohesionless material during the general landslide. These authors also mention that the maximum force experienced by the shear pile wall probably ranged between 800 and $900\ kN/m$. As a result, residual strength parameters retained in the present study were

$c'_{res} \approx 0$, $\phi'_{res} = 20°$. These yield $F = 0.74$ from Eq. (2b). In addition, substitution of $F = 1$ in this equation leads to $z_{lim} = 3.23m$. Eq. (11) was used to compute total passive pressure σ_{rp} for $z > z_{lim}$. The total passive pressure σ_{rp} and the corresponding force F_{rp} are reported in Fig. 9. The total passive force $F_{rp} = 529.71kN/m$. The length of slope L' required to mobilize the force F_{rp} equals $55.05m$ from Eq. (12), because the shear stress deficit $\Delta\tau = 9.62\ kPa$ at $H = 7m$. The additional length $L_B = C_1C_2 + C_2C = 10.74 + 2.47 \cong 13.21m$. Indeed, the length of segment C_1C_2 was determined by assuming that the slip line B'A_1 in Fig. 6 is an arc of circle, whereas the length of segment C_2C was found from Eq. (14). Thus, the critical length $L_{crit} = L' + L_B \cong 68.26m$, which is less than the actual length L of $110m$ of the landslide. As a consequence, the sliding mass would pass over the crest of the wall, as it eventually occurred. In addition, the maximum force $F_p = F_{rp} + \Delta\tau L_B$ or $657\ kN/m$ approximately, as shown in Fig. 10. Failure was thus inevitable, because the wall was designed to withstand an ultimate load of $590\ kN/m$, which corresponds to a factor of safety $F = 590/657$ or about 0.9. This notwithstanding, the expected maximum force of $657\ kN/m$ is much smaller than the value of 800 and $900kN/m$ deduced by Blondeau and Virollet [26]. It is believed that the aggravating factor which led to the failure of the shear pile wall was the fact that the piles were not all anchored in the bedrock.

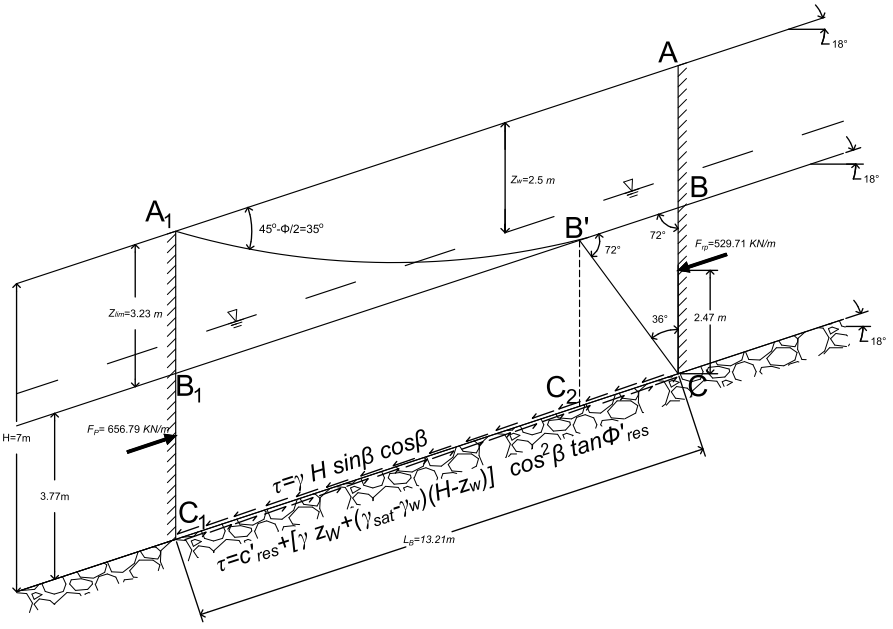

Fig. 10. Free-body diagram at passive end of landslide.

4. Conclusions

The following conclusions are drawn on the basis of various points discussed in the paper.

a) Guidelines are given for the safe design of earth retention systems installed at the toe of unstable slopes.
b) Infinite analyses are combined with the slip line solution of Résal [23] and Frontard [24] for a better understanding of the mechanism mobilized in long landslides.
c) A case history involving a long landslide is re-analyzed and is shown that, in spite of the presence of a massive shear pile wall, failure was to be expected.

CRediT authorship contribution statement

Ghassan Abou-Samra: Methodology, Investigation, Formal analysis, Conceptualization. **Vincenzo Silvestri:** Methodology, Conceptualization.

Declaration of competing interest

The authors declare that they have no known competing financial interests or personal relationships that could have appeared to influence the work reported in this paper.

Data availability

No data was used for the research described in the article.

References

[1] R.D. Holtz, R.L. Schuster, Stabilization of soil slopes, in: A.K. Turner, R.L. Schuster (Eds.), Special Report 247, Landslides: Investigation and Mitigation, vol. 5, Transportation Research Board, Washington, Ch, 1996, pp. 439–473.
[2] M.E. Popescu, K. Sasahara, Engineering measures for landslide disaster mitigation, in: K. Sassa, P. Canuti (Eds.), Landslide Disaster Risk Reduction, vol. 32, Springer-Verlag, Berlin, Ch, 2009, pp. 609–631.
[3] D.H. Cornforth, Landslides in Practice: Investigation, Analysis, and Remedial/preventative Options in Soils, Wiley, Hoboken, New Jersey, 2005.
[4] T. Carlà, R. Macciotta, M. Hendry, D. Martin, T. Edwards, T. Evans, P. Farina, E. Intrieri, N. Casagli, Displacement of a landslide retaining wall and application of an enhanced failure forecasting approach, Landslides 15 (2018) 489–515.
[5] J.M. Duncan, S.G. Wright, Soil Strength and Slope Stability, John Wiley and Sons, Inc., New York, 2005.
[6] B.M. Das, K. Sobhan, Principal of Geotechnical Engineering, 10, Cengage Learning, Boston, Massachusetts Hoboken, New Jersey, 2016 th Edn.
[7] T.W. Lambe, R.V. Whitman, *Soil Mechanics*, 1, John Wiley & Sons, New York, 1969 st Edn.
[8] D.W. Taylor, Fundamentals of Soil Mechanics, 1, John Wiley & Sons, New York, 1948 st Edn.
[9] W.J.M. Rankine, On the Stability of Loose Earth, vol. 147, Transactions of the Royal Society of London, 1857, pp. 9–27.
[10] W.C. Huntington, Earth Pressures and Retaining Walls, John Wiley & sons, New York, 1957.
[11] D. Griffiths, J. Huang, G.F. Dewolfe, Numerical and analytical observations on long and infinite slopes, Int. J. Numer. Anal. Methods GeoMech. 35 (5) (2011) 569–585.
[12] S. Feng, R.H. Huang, L.T. Zhan, H.W. Liu, Semi-analytical solution of pore-water pressure in unsaturated ground and infinite slope considering highly nonlinear soil hydraulic properties, Comput. Geotech. (2023), https://doi.org/10.1016/j.compgeo.2023.105795.
[13] R.M. Iverson, Landslides triggering by rain infiltration, Water Resour. Res. 36 (7) (2000) 1897–1910.
[14] J. Yang, On Seismic landslide hazard assessment, Geotechnique 57 (8) (2007) 707–713.
[15] J.A.M. Teunissen, S.E.J. Spierenburg, Stability of infinite slopes, Geotechnique 45 (2) (1995) 321–323.
[16] G. Urciuoli, M. Pirone, L. Picarelli, Considerations on the mechanics of failure of the infinite slope, Comput. Geotech. 107 (2019) 68–79, https://doi.org/10.1016/j.compgeo.2018.11.008, 2019.
[17] B. Van den Bout, L. Lombardo, M. Ghiyang, C.J. van Westen, V. Jetten, Physically-based catchment-scale prediction of slope failure volume and geometry, Eng. Geol. 284 (2021) 105942.
[18] R.L. Michalowski, Failure potential of infinite slopes in bonded soils with tensile strength cut-off, Can. Geotech. J. 55 (4) (2018) 477–485.
[19] D. Park, Infinite rock slope analysis with Hoek-Brown failure criterion, Rock Mech. Rock Eng. 56 (2023) 6919–6928, https://doi.org/10.1007/s00603-023-03431-y, 2023.
[20] D. Park, Implications of the infinite rock slope analysis: tension cut-off and graphical interpretation, Comput. Geotech. (2024), https://doi.org/10.1016/comgeo.2024.106410.
[21] A. Serrano, C. Olalla, J. Manzanas, Stability of highly fractured infinite rock slopes with nonlinear failure criteria and nonhomogeneous flow laws, Can. Geotech. J. 42 (2) (2005) 393–411.
[22] V. Silvestri, C. Tabib, Failure of a shear pile wall used for the stabilization of a long landslide, in: S. Aversa, L. Cascini, L. Picarelli, C. Scavia (Eds.), Proceedings of the 12th International Symposium on Landslides (Napoli, Italy, 12-19 June 2016), Landslides and Engineered Slopes. Experience, Theory and Practice, Taylor & Francis Group, London, 2016, https://doi.org/10.1201/9781315375007. CRC Press.
[23] J. Résal, Poussée des terres. Deuxième partie. *Théorie des terres cohérentes.* Librairie Polytechnique, Ch. Béranger, 1910. Paris.
[24] M. Frontard, Cycloïdes de glissement des terres. Comptes rendus hebdomadaires de l'Académie des sciences, Bacheliers, Paris, 1922, pp. 526–529.
[25] G. Sanglerat, G. Olivari, B. Cambou, Problèmes pratiques de mécanique des sols et de fondations. Tome vol. 1, Dunod, Paris, 1980.
[26] F. Blondeau, M. Virollet, Comportement des murs de soutènement en zone instable, in: Stabilité des talus, 1 : versants naturels. Bulletin de Liaison des Ponts et Chaussées, Numéro spécial II, 1976, pp. 149–154.
[27] F. Blondeau, H. Josseaume, Mesure de la résistance au cisaillement résiduelle en laboratoire, in: Stabilité des talus, 1 : versants naturels. Bulletin de Liaison des Ponts et Chaussées, Numéro spécial II, 1976, pp. 90–106.